AGU PUBLICATIONS

Geophysical Research Letters

RESEARCH LETTER
10.1002/2017GL075370

Key Points:
- MPI-ESM large ensemble simulates negative and positive decadal trends of carbon uptake in the current and the future ocean
- Largest internal variability in the ocean carbon uptake is found in the Southern Ocean, the North Pacific, and the North Atlantic
- The Southern Ocean and North Pacific require the largest number of ensembles from 46 to 79 to capture decadal forced (ensemble mean) signal

Supporting Information:
- Supporting Information S1

Correspondence to:
H. Li,
hongmei.li@mpimet.mpg.de

Citation:
Li, H., & Ilyina, T. (2018). Current and future decadal trends in the oceanic carbon uptake are dominated by internal variability. *Geophysical Research Letters*, *45*, 916–925. https://doi.org/10.1002/2017GL075370

Received 21 AUG 2017
Accepted 20 DEC 2017
Accepted article online 27 DEC 2017
Published online 17 JAN 2018

Current and Future Decadal Trends in the Oceanic Carbon Uptake Are Dominated by Internal Variability

Hongmei Li[1] **and Tatiana Ilyina**[1]

[1]Max Planck Institute for Meteorology, Hamburg, Germany

Abstract We investigate the internal decadal variability of the ocean carbon uptake using 100 ensemble simulations based on the Max Planck Institute Earth system model (MPI-ESM). We find that on decadal time scales, internal variability (ensemble spread) is as large as the forced temporal variability (ensemble mean), and the largest internal variability is found in major carbon sink regions, that is, the 50–65°S band of the Southern Ocean, the North Pacific, and the North Atlantic. The MPI-ESM ensemble produces both positive and negative 10 year trends in the ocean carbon uptake in agreement with observational estimates. Negative decadal trends are projected to occur in the future under RCP4.5 scenario. Due to the large internal variability, the Southern Ocean and the North Pacific require the most ensemble members (more than 53 and 46, respectively) to reproduce the forced decadal trends. This number increases up to 79 in future decades as CO_2 emission trajectory changes.

1. Introduction

Signatory countries of the 2015 Paris Agreement agreed to avoid global warming exceeding 2°C above preindustrial levels by curbing their fossil fuel CO_2 emissions (United Nations Framework Convention on Climate Change, 2015). One major requirement related to this goal will be to discern the pathways of anthropogenic carbon in the Earth system in order to verify the effectiveness of fossil fuel emissions reduction measures (Marotzke et al., 2017). A major scientific challenge in this regard is to infer the interannual and decadal variations of the ocean carbon sink, as well as its susceptibility to ongoing climate change (Ilyina, 2016; Ilyina & Friedlingstein, 2016; Peters et al., 2017).

The oceans currently absorb about 25–30% of anthropogenic carbon emissions (Le Quéré et al., 2017) and thereby modulate the response of the Earth system to climate change. Observations (Fay & McKinley, 2013; Landschützer et al., 2015; Schuster & Watson, 2007) have revealed pronounced decadal variations occurring along with decreasing ocean carbon uptake for the period from 1992 to 2001. Data-based estimates of oceanic carbon uptake show large uncertainties arising from the gaps in observations and different mapping methods that are used to derive observational products (Rödenbeck et al., 2015). Earth system models (ESMs), driven by future climate change scenarios, that is, those used in the fifth Phase of the Coupled Model Intercomparison Project (CMIP5), project an increase in the ocean carbon uptake in the recent decades and into the future, as long as CO_2 emissions increase (Frölicher et al., 2016; Nevison et al., 2016; Wang et al., 2016). Yet large discrepancies appear among these model simulations due to uncertainties related to internal variability, model response, and scenarios (Deser et al., 2012; Hawkins & Sutton, 2009; Lovenduski et al., 2016; Tebaldi & Knutti, 2007). Model simulations, based on decadal prediction systems (Li et al., 2016), large ensemble simulations (McKinley et al., 2016, 2017), CMIP5 multimodel preindustrial control simulations (Resplandy et al., 2015), and ocean stand-alone models (Thomas et al., 2008) indicate large interannual to decadal variations of the ocean carbon sink in major carbon sink/source regions. This internal variability of the Earth system interferes with the detection of the direct response of the ocean carbon sink to increasing anthropogenic carbon emissions (Keller et al., 2014; McKinley et al., 2016; Séférian et al., 2014). Thus, the contribution of internal variability to the ocean carbon uptake uncertainty, and the future evolution of this internal variability remain poorly quantified. Moreover, as of now, CMIP5 historical simulations are not expected to reproduce the decreasing decadal trends in the ocean carbon uptake during 1992–2001 (Wang et al., 2016) as found in observational estimates. Hindcast models forced with atmospheric reanalysis may better capture decadal variations of the ocean carbon uptake driven by climate variability.

ESM-based perturbed initial conditions ensembles allow for a consistent evaluation of both forced signals and internal variability within the same model. The important role of internal climate variability for projections of ocean biogeochemistry has been already confirmed, using such ensembles (containing 30 members) (Lovenduski et al., 2016; McKinley et al., 2016; Rodgers et al., 2015). Ensuring that ESMs can reasonably simulate the actual variations of the present-day ocean carbon sink, along with the trend in response to anthropogenic forcing, is critical for future climate change projections. Moreover, understanding of natural variability is necessary for establishing robust prediction skill of the ocean carbon sink (Li et al., 2016). As shown in previous studies (Deser et al., 2012; Frölicher et al., 2016; Keller et al., 2014; Lovenduski et al., 2016; Rodgers et al., 2015), internal variability dominates forced trend on time scales of several decades. Emergence of the forced trend on decadal time scales from the internal variability depends on the number of ensemble members. We use a large ensemble of 100 historical and future (following the moderate emission scenario RCP4.5) simulations based on Max Planck Institute Earth system model (MPI-ESM) to investigate the ocean carbon uptake variability. This ensemble has already been documented in previous studies focusing on various features of the physical climate system (Bittner et al., 2016; Hedemann et al., 2017; Stevens, 2015; Suárez-Gutiérrez et al., 2017). Here we address the following questions: (1) Can the ensemble reproduce the occurrence of negative and positive decadal trends in the air-sea CO_2 fluxes detected in observations in major carbon sink/source regions? (2) How many ensemble members are required to capture the forced signal over decadal timeframes?

Here the 100-member ensemble mean is defined as the "forced" trend, such as the trend produced by both, natural and anthropogenic forcings including CO_2 emissions. The difference between single-member outcomes and the ensemble mean represents the internal variability or "unforced" trend (Deser et al., 2014; Ting et al., 2009).

2. Methods

2.1. Model Description

The MPI-ESM version 1.1 in a low-resolution configuration (MPI-ESM-LR) is used for the large ensemble simulations. It has an incremental improvement of the energy conservation in the atmospheric component ECHAM6 (Popp et al., 2016) compared to the CMIP5 model (Giorgetta et al., 2013). ECHAM6 has a horizontal resolution of T63/1.9° and 47 vertical levels (Stevens et al., 2013). The ocean component Max Planck Institute Ocean Model (MPIOM) has a horizontal resolution of 1.5° on average and 40 vertical levels (Jungclaus et al., 2013). The Hamburg Ocean Carbon Cycle Model (HAMOCC) (Ilyina et al., 2013) is implemented into the MPIOM and represents the ocean biogeochemistry component of MPI-ESM. The land carbon cycle is represented by the model JSBACH (Reick et al., 2013).

An ensemble of 100 members for the historical simulations, extended by Representative Concentration Pathways scenarios RCP4.5 has been conducted for the periods spanning the years 1850–2005 and 2006–2100, respectively. The ensemble members are generated by starting the historical simulations in year 1850 from different years, with a random time interval, of the preindustrial control simulation. Thereby, we subsample the full range of internal variability in the preindustrial control states of the model. Note that there are different ensemble generation techniques (Kay et al., 2015; McKinley et al., 2016; Rodgers et al., 2015) and the memory of initial perturbation vanishes in about a decade (Branstator & Teng, 2010; Kirtman et al., 2013). The subsampled internal variability, which is generally independent to the ensemble generation methods in several decades after the initialization, is inevitably model dependent.

2.2. Observational Data

For comparison with model simulations, we use 10 data-based estimates of the global oceanic carbon flux from the Surface Ocean pCO_2 Mapping intercomparison (SOCOM, Rödenbeck et al., 2015). All these data products are based on the surface ocean CO_2 atlas version 2 (SOCATv2) (Bakker et al., 2014) or the Lamont-Doherty Earth Observatory version 2013 (LDEOv2013) (Takahashi et al., 2014) databases. Different methods are used to fill the spatiotemporal gaps in observations and to obtain a global coverage of the ocean surface carbon uptake. The spatial distribution of CO_2 flux was only available for three SOCOM products, that is, SOM-FFN (Landschützer et al., 2016), Jena-MLS (Rödenbeck et al., 2013), and JMA-MLR

(Iida et al., 2015). The uncertainty of SOM-FFN data-based estimate (Landschützer et al., 2014, 2015, 2016) is used to further evaluate our model simulations.

2.3. Statistical Analyses

The modeled air-sea CO_2 fluxes are interpolated from the original curvilinear grid to a 1° grid for comparison with the data-based estimates, which are likewise available on a 1° × 1° grid. In this study, the ocean regions are defined as follows: the North Atlantic Ocean (80°W–60°E, 30°N–80°N), the North Pacific Ocean (110°E–90°W, 30°N–80°N), the Tropical Ocean (30°S–30°N), and the Southern Ocean (to the south of 30°S). Annual mean values are used here for further statistical analysis. Here primarily focus on the anomalous CO_2 flux time series (as shown in Figure 1) which is computed by removing the climatological mean. The climatological mean indicates the long-term mean which spans the years 1982–2011 for the model simulations, and the available time period mean for the data-based estimates.

We use the analysis of variance (ANOVA) method to quantify the relative amplitude of internal variability (spread of the ensemble members referring to the ensemble mean time series) in comparison to the forced temporal variability (standard deviation of the ensemble mean time series). Details of this method can be found in the supporting information (Harzallah & Sadourny, 1995; Ting et al., 2009; Zhou & Yu, 2006). Linear decadal (i.e., 10 year) trends are calculated using a least squares regression method. Here a negative trend indicates a weakening of the ocean carbon sink or an enhancement of the outgassing of CO_2 from the ocean, and vice versa for the positive trend. For each 10 year period, we count how many ensemble members produce a negative trend.

To estimate how many ensemble members are needed to capture the forced trends in the presence of the internal variability on decadal timescales, we use the 100-member mean as a reference and calculate the spatial correlation of the mean trend in CO_2 flux for different ensemble sizes against 100-member ensemble mean trend. For different ensemble sizes, we use a bootstrap method to calculate the correlation 1,000 times based on different combinations of randomly chosen ensemble members (details can be found in the supporting information).

3. Occurrence of Negative and Positive Trends in the Ocean Carbon Uptake

For the evaluation of the historical ocean carbon uptake, we focus on the recent 30 years (i.e., 1982–2011) during which ocean surface observational data are available. Note that the climatological mean state of air-sea CO_2 fluxes from model simulations is somewhat higher than the SOCOM data products which is common for CMIP5 models (Ilyina, 2016). Spatially, the MPI-ESM model captures the climatology structure of the oceanic CO_2 uptake (Figure S1). The discrepancy in the Southern Ocean is consistent with the CESM large ensemble and CMIP5 multimodel simulations as shown by McKinley et al. (2016).

Although a positive trend prevails in the ensemble mean (Figure 1), the oceanic carbon uptake shows large internal variability, represented by the spread among the 100 ensemble members. Likewise, the data-based products also show a large spread due to the sparse spatiotemporal coverage of observations and different data mapping methods (Rödenbeck et al., 2015). The internal variability (calculated based on the ANOVA method; see section 2.3) of the MPI-ESM simulations (0.14 Pg C yr^{-1}) is in the envelope of the observation-based estimates, that is, the uncertainty of the 10 SOCOM data products (0.18 Pg C yr^{-1}). This suggests that the large ensemble is able to capture the range of the uncertainty suggested by observation. In general, the internal variability is as large as the forced temporal variability in MPI-ESM large ensemble simulations, and the internal variability (0.04 and 0.14 Pg C yr^{-1}) is even larger than the forced temporal variability (0.02 and 0.12 Pg C yr^{-1}) in major carbon sink regions such as the North Pacific and the Southern Ocean, respectively (Table 1). The internal variability of outgassing and uptake CO_2 fluxes in different regions cancels each other and leads to a dominant signal of the forced variability in the globally integrated ocean carbon uptake. This imposes challenges on the detection of the forced signal from a single or a few ensemble-member simulations over the last 30 years.

Despite growing CO_2 emissions, the uptake of carbon by the ocean decreased in many ocean regions in the 1990s and increased again in the 2000s (Landschützer et al., 2015; McKinley et al., 2017; Schuster & Watson, 2007). This feature is captured in most SOCOM products and is related to natural variability of the climate system. In the SOM-FFN data set, 50% of the increase in the ocean carbon sink after 2000 occurs in the Southern

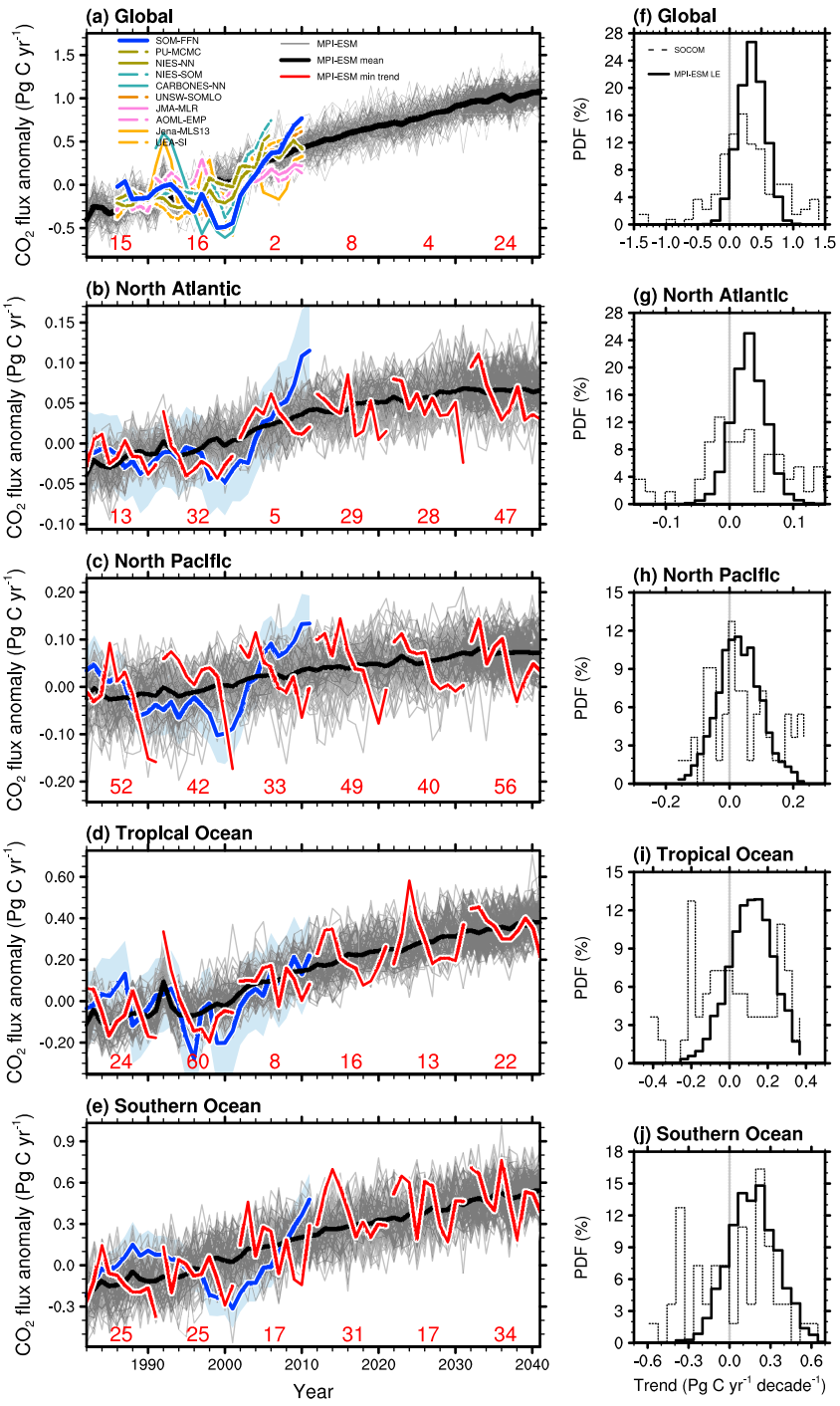

Figure 1. Anomalous air-sea CO_2 flux in the global ocean and different ocean basins. (a–e) Historical and near-future (under RCP4.5 scenario) evolution of anomalous air-sea CO_2 flux from data-based estimates and MPI-ESM 100-member ensemble simulations. Positive values indicate carbon flux into the ocean. The gray curves in Figures 1a–1e show individual ensemble members and black thick curves show the ensemble mean. Color lines in Figure 1a shows 10 data-based estimates from different observational products (SOCOM, Rödenbeck et al., 2015). The blue curves and light blue shading in Figures 1b and 1c show the SOM-FFN data and its uncertainty (Landschützer et al., 2016). The red curves in Figures 1b–1e show members with the smallest trends in the respective decades. The red numbers show the number of ensemble members producing negative trends in these decades. (f–j) PDF of decadal trends in the global and regional ocean CO_2 uptake from the MPI-ESM large ensemble simulations during the period from 1982 to 2011 (solid line) and from SOCOM available data products (dashed line). The available three SOCOM products, that is, SOM-FFN, Jena-MLS, and JMA-MLR, are used for the PDF statistics of the regional oceans (Figures 1g–1j). Here we use all the available 10-year trends during the period from 1982 to 2011 from these three data products. The gray vertical line on PDF plots shows the zero trend.

Table 1
Variability of Global and Regional Integrated CO_2 Flux Based on the Time Series From MPI-ESM Large Ensemble Simulation for the Period From 1982 to 2011 (Time Series See Figure 1)

	Variability (in Pg C yr^{-1})	
	Internal	Forced
Global Ocean	0.14	0.24
North Atlantic	0.02	0.02
North Pacific	0.04	0.02
Tropical Ocean	0.07	0.08
Southern Ocean	0.14	0.12

Note. The variabilities are calculated based on the ANOVA analysis (see section 2).

Ocean (Landschützer et al., 2015, 2016). Even in the presence of large uncertainty due to sparse data, the SOCOM data sets show agreement in decadal variations of the Southern Ocean carbon uptake (Ritter et al., 2017). The ensemble spread values of the air-sea CO_2 flux in MPI-ESM are of the same magnitude as the uncertainty of the SOM-FFN data. However, the ensemble mean does not capture the decrease in the ocean carbon sink in the 1990s as implied by observational products. This is not surprising, as variations of the climate system in such free ESM simulations started in 1850 and running without data assimilation do not evolve synchronously with the observed climate variability. However, can individual ensemble members capture decadal decreasing trends in the ocean carbon uptake that are implied by observations?

Our analysis shows that a large number of ensemble members produce negative trends in the air-sea CO_2 flux for each 10 year time window (shown with the red numbers in Figure 1). For instance, 25, 42, and 60 members show negative trends during the years 1992–2001 in the Southern Ocean, the North Pacific, and the Tropical Ocean, respectively (Figure 1). The Probability Density Function (PDF) of the decadal trends in the period from 1982 to 2011 (Figures 1f–1j) indicates that the simulated trends are skewed toward positive values due to the increase of anthropogenic carbon emissions; nevertheless, a number of ensemble members show negative trends which are found in observations. The PDF of global ocean carbon uptake from MPI-ESM large ensemble has a smaller range of trends than the SOCOM products. In the regional oceans, PDF distribution of SOCOM products shows more scattered structure, likely due to a small sample size. In the North Pacific, several ensemble members produce negative decadal trends that are comparable to the negative trends calculated from SOCOM data-based estimates. The air-sea CO_2 flux peaks in the 1983 and 1992 in most of the ocean areas, which is related to the effects of volcanic eruptions (Ding et al., 2014; Frolicher et al., 2011, 2013; Segschneider et al., 2013).

The internal variability of 10 year trends in the MPI-ESM ensemble is still large in the future projections in all analyzed ocean regions (Figure 1). Interestingly, despite the growing atmospheric CO_2 concentration prescribed in the RCP4.5 scenario, a large number of ensemble members still project decadal negative trends in the future. The number of ensemble members reproducing decadal negative trends varies from decade to decade (Table S1). Moreover, beyond the year 2040, the number of ensembles with negative trends tends to increase. This is related to the temporal evolution of fossil fuel CO_2 emissions in the RCP4.5 scenario, which stabilized around 2040 and start decreasing thereafter (van Vuuren et al., 2011). This implies that internal climate variations will continue modulating the ocean carbon sink and that decadal decreasing trends will occur in the background of increasing CO_2 emissions that drive the long-term growth of the ocean carbon sink.

4. Spatial Distributions of Trends in the Ocean Carbon Uptake

Variations in the air-sea CO_2 flux show pronounced regional features during the years 1992–2001 (Figure 2). The forced trends (in response to both the natural and anthropogenic forcings), represented by the 100 ensemble member mean (Figure 2c), show large-scale spatial structures with positive trends (i.e., increasing carbon uptake) in major carbon sink areas such as the Southern Ocean, the North Atlantic, and the North Pacific. The ensemble shows large internal variability (Figure 2f). The spread of air-sea CO_2 flux trend in the Southern Ocean and the North Pacific is larger than 1.0 g C m^{-2} yr^{-2}, which is about twice as large as the forced trends shown in Figure 2c. This implies that the trends induced by natural climate variability can be as large as the trends due to external forcing including atmospheric CO_2 concentration over a given decade.

The amplitude of internal variability in trends of the air-sea CO_2 flux can be illustrated using extreme cases, in particular, using the ensemble members with the smallest and largest trends during the years 1992–2001 (Figures 2a and 2d). In the ensemble member with the smallest trend in the global ocean carbon uptake, negative trends are found along the 50–65°S latitude of the Southern Ocean, and positive trends are found in the North Pacific. This is reversed in the ensemble member with the largest trend in the global ocean carbon uptake. The opposing signs of the regional trends in the simulations with the largest and the smallest

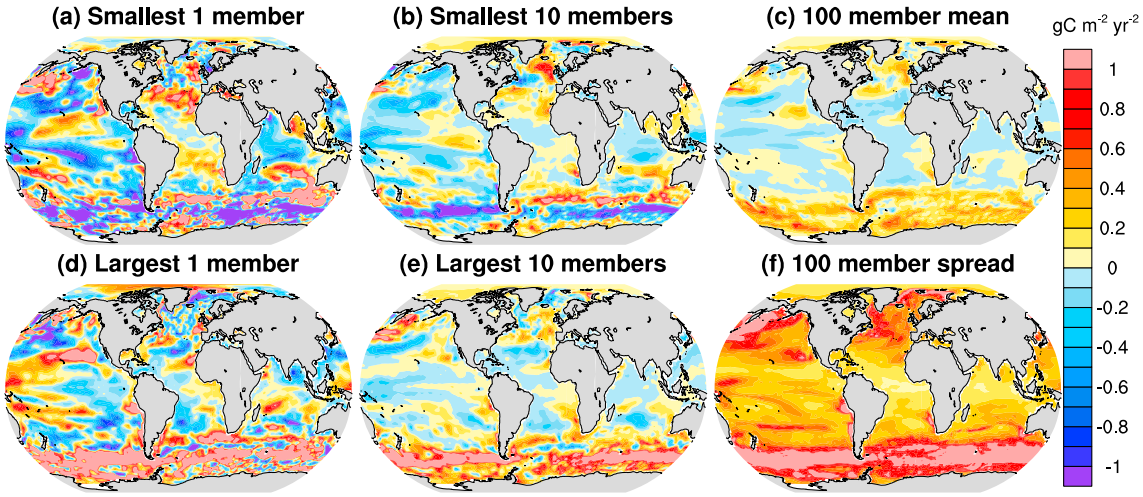

Figure 2. Spatial distribution of trends in the air-sea CO_2 flux during the period 1992–2001 based on varying ensemble size. (a and d) The single-member results with the smallest and the largest trend of the global integrated carbon sink. (b and e) The 10-member ensemble mean results with the smallest and the largest trends. The 100-member (c) ensemble mean and (f) standard deviation of the decadal trend. Note a negative trend indicates that the ocean carbon uptake is weakening.

trends remain prominent even in the 10-member mean (see Figures 2b and 2e). Moreover, variations in the global ocean carbon uptake are dominated by its variations in the Southern Ocean. Variations of the ocean carbon uptake are related to the background thermal and dynamical changes, predominantly by changes in the atmospheric forcing, as indicated in previous studies (Landschützer et al., 2015; Le Quéré et al., 2009). In our analysis, this is manifested by the reversal of trends in the 10 m wind and sea level pressure in the ensemble members with smallest/largest trends (Figure S2).

5. The Necessary Ensemble Size to Infer Decadal Variations of the Ocean Carbon Uptake

How many ensemble members are enough to reproduce the forced trend and the internal variability in different ocean regions over a variety of 10 year periods? To address this question, we take the 100-member ensemble mean as a reference and calculate the spatial correlation of the ensemble mean trends for a varying number of members in relation to the reference field (Figures 3a and S3). The correlation increases with an increasing number of ensemble members. To reproduce the forced trend at the correlation level of 0.9 with the reference ensemble mean field in the decade 1992–2001, the North Atlantic Ocean and the Tropical Ocean requires less members, that is, 40 and 43, respectively, and the Southern Ocean and the North Pacific Ocean require more, that is, 56 ensemble members (see Table S2). The larger required ensemble size is consistent with the larger internal variability found in the Southern Ocean and the North Pacific Ocean in our simulations (Figure 2 and Table 1). For the global ocean, 45 ensemble members are required to produce the forced decadal trend of ocean carbon uptake in the presence of large internal variability during 1992–2001. We also calculate correlations based on references of single member trends (Figure S4). The correlation is quite low, indicating that with regard to decadal trends, the ensemble members are relatively independent of each other.

The temporal evolution of the required ensemble members to represent the forced trends varies largely from decade to decade, which indicates a nonsteady internal variability (Figure 3b). For all analyzed ocean regions and global integration, more ensemble members are necessary at the end of the simulation in 2080s relative to 1980s. This implies a tendency of increase in internal variability with time under RCP4.5 scenario. For instance, globally the number varies from 45 currently to 71 in the future. Regionally, the North Pacific and the Southern Ocean requires more ensemble members (being 46 and 53 in current decades up to 79 and 76 in the future, respectively) than other regions due to the large internal variability prone to these regions. The increase in internal variability is related to changes in the temporal evolution of CO_2 emissions which level off in the RCP4.5 scenario in the 2040s. This feature has not been addressed in previous studies focusing mainly on the high CO_2 scenario RCP8.5 (Deser et al., 2016; McKinley et al., 2016; Rodgers et al., 2015).

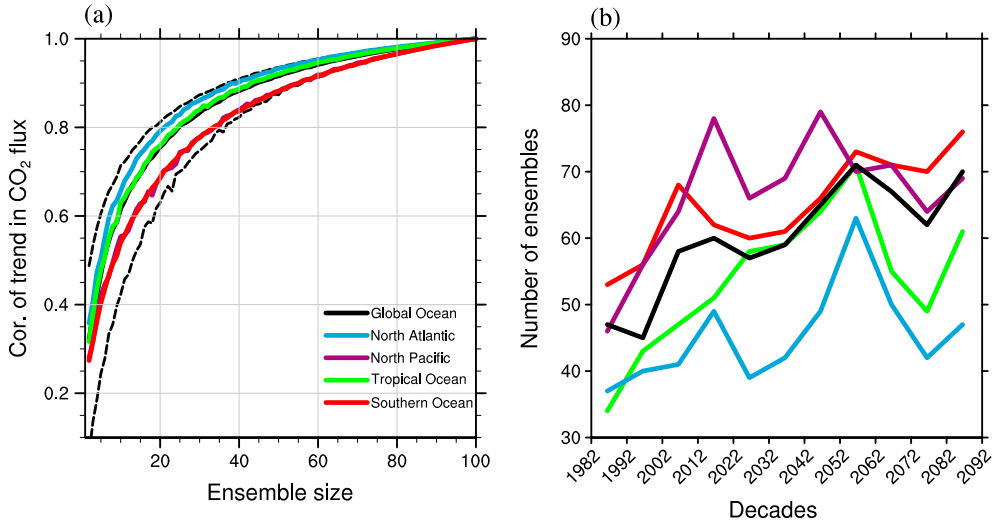

Figure 3. (a) Spatial correlation of the mean trend in the CO_2 flux for different ensemble size against 100-member ensemble mean trend in the global (black line) and different ocean regions (color lines) during the decade from 1992 to 2001. For each ensemble size, the correlation coefficient is calculated 1,000 times using a bootstrap resample method. The solid lines show the mean results. Here we only show the 90% confidence interval (i.e., 5–95% of the ranked correlations from the 1,000 resampled results) for the global ocean. (b) Temporal evolution of the ensemble members required to produce high spatial correlation of 0.9 with the 100-member mean trend pattern in different ocean regions. The *x* axis shows the consecutive decades, and the *y* axis shows the necessary ensemble members for respective decade.

6. Summary and Conclusions

The internal variability of the air-sea CO_2 flux simulated by the 100-member MPI-ESM ensemble is as large as the forced temporal variability on decadal timescales. We find that various ensemble members produce both positive and negative decadal (i.e., 10 year) trends during the past decades. This feature of the MPI-ESM large ensemble is of particular interest because negative trends in the global ocean carbon uptake have been detected in observational estimates over the years 1992–2001, but it is especially challenging for free simulations with ESMs to capture them. Furthermore, both positive and negative decadal trends in global ocean carbon uptake occur in the future. While positive decadal trends are expected due to rising CO_2 emissions as suggested by model projections (Lovenduski et al., 2016; McKinley et al., 2016), the occurrence of negative trends implies that climate variability will also play a prominent role in determining the near-future ocean carbon sink. Moreover, the number of ensemble members which produce negative trends remains relatively constant as atmospheric CO_2 concentrations grow. This implies that the monitoring systems designed to verify the fate of anthropogenic emissions and the mitigation measures put in place in the aftermath of the 2015 Paris Agreement will have to account for the strong variability in the ocean carbon sink. Continuous efforts such as SOCAT (Bakker et al., 2016) are crucial to provide an observational basis for determining the internal variability in oceanic carbon uptake.

Regionally, the largest variability of decadal trends in the air-sea CO_2 flux is found in the 50–65°S band of the Southern Ocean, the North Atlantic, and the North Pacific. Our analysis suggests that a different number of ensemble members are required to reproduce variability in different ocean regions. Due to large internal variability, more than 45 ensemble members are necessary during current decades and in the future for the global ocean carbon sink to reproduce the spatial pattern of the decadal forced trend with the correlation of 0.9. Regionally, the Southern Ocean and the North Pacific require the largest ensemble size (more than 53 and 46, respectively). The required number of ensemble members varies from decade to decade and is up to 79 in the future. Hence, large ensembles are required for the forced signal to emerge from the internal variability on decadal timescale in model projections. As the trajectories of oceanic carbon uptake vary in different emission scenario, the forced trend may emerge faster in high emission RCP8.5 scenarios (Lovenduski et al., 2016; McKinley et al., 2016; Rodgers et al., 2015) than in moderate emission RCP4.5 scenario.

We note that our estimates of internal variability of air-sea CO_2 fluxes may be affected by the given model configuration. For instance, as shown in previous studies (Li & von Storch, 2013; Penduff et al., 2011), internal variability of buoyancy fluxes and sea level induced by stochastic processes may be suppressed in low resolution model configurations. Furthermore, a simulation with interactive carbon cycle, driven by CO_2 emissions projected a 25% higher variability than the one driven by atmospheric CO_2 concentrations (Ilyina et al., 2013).

As shown in a previous study (Resplandy et al., 2015), the internal variability of the air-sea CO_2 flux is not necessarily consistently captured in ESM simulations. The diversity in modeled variability is needed to reproduce the evolution of reality, as observed changes could be just one realization or a superposition of several realizations of the ensemble simulation. Multimodel intercomparison studies based on large ensemble simulations are essential for further understanding of the origins of the differences among the models in producing the internal variability.

Acknowledgments
We acknowledge funding from the Federal Ministry of Education and Research in Germany (BMBF) through the research programme "MiKlipII" (FKZ: 01LP1517B). This study has also received funding from the European Union's Horizon 2020 research and innovation programme under grant agreement No 641816. We acknowledge Peter Landschützer and Christian Rödenbeck for providing the SOM-FFN and SOCOM data and acknowledge Yohei Takano, Jochem Marotzke, Nicola Maher, Sebastian Milinski, and Irene Stemmler for their helpful comments on this paper. Thanks to Frank Sienz for his expertise on statistics of this study. Thanks to Luis Kornblueh, Jürgen Kröger, Michael Botzet, and Irene Stemmler for making the large ensemble simulations available. The simulations were performed at the Swiss national supercomputing center (CSCS) and the German Climate Computing Center (DKRZ). Primary data and scripts used in the analysis of this study are archived by the Max Planck Institute for Meteorology and can be obtained by contacting publications@mpimet.mpg.de.

References

Bakker, D. C. E., Pfeil, B., Landa, C. S., Metzl, N., O&'Brien, K. M., Olsen, A., … Xu, S. (2016). A multi-decade record of high quality fCO_2 data in version 3 of the Surface Ocean CO_2 Atlas (SOCAT). *Earth System Science Data*, *8*(2), 383–413. https://doi.org/10.5194/essd-8-383-2016

Bakker, D. C. E., Pfeil, B., Smith, K., Hankin, S., Olsen, A., Alin, S. R., … Watson, A. J. (2014). An update to the Surface Ocean CO_2 Atlas (SOCAT version 2). *Earth System Science Data*, *6*(1), 69–90. https://doi.org/10.5194/essd-6-69-2014

Bittner, M., Schmidt, H., Timmreck, C., & Sienz, F. (2016). Using a large ensemble of simulations to assess the Northern Hemisphere stratospheric dynamical response to tropical volcanic eruptions and its uncertainty. *Geophysical Research Letters*, *43*, 9324–9332. https://doi.org/10.1002/2016GL070587

Branstator, G., & Teng, H. (2010). Two limits of initial-value decadal predictability in a CGCM. *Journal of Climate*, *23*(23), 6292–6311. https://doi.org/10.1175/2010JCLI3678.1

Deser, C., Phillips, A. S., Alexander, M. A., & Smoliak, B. V. (2014). Projecting North American climate over the next 50 years: Uncertainty due to internal variability. *Journal of Climate*, *27*(6), 2271–2296. https://doi.org/10.1175/JCLI-D-13-00451.1

Deser, C., Phillips, A., Bourdette, V., & Teng, H. (2012). Uncertainty in climate change projections: The role of internal variability. *Climate Dynamics*, *38*(3-4), 527–546. https://doi.org/10.1007/s00382-010-0977-x

Deser, C., Terray, L., & Phillips, A. S. (2016). Forced and internal components of winter air temperature trends over North America during the past 50 years: Mechanisms and implications. *Journal of Climate*, *29*(6), 2237–2258. https://doi.org/10.1175/JCLI-D-15-0304.1

Ding, Y. N., Carton, J. A., Chepurin, G. A., Stenchikov, G., Robock, A., Sentman, L. T., & Krasting, J. P. (2014). Ocean response to volcanic eruptions in Coupled Model Intercomparison Project 5 simulations. *Journal of Geophysical Research: Oceans*, *119*, 5622–5637. https://doi.org/10.1002/2013JC009780

Fay, A. R., & McKinley, G. A. (2013). Global trends in surface ocean pCO_2 from in situ data. *Global Biogeochemical Cycles*, *27*, 541–557. https://doi.org/10.1002/gbc.20051

Frolicher, T. L., Joos, F., & Raible, C. C. (2011). Sensitivity of atmospheric CO_2 and climate to explosive volcanic eruptions. *Biogeosciences*, *8*(8), 2317–2339. https://doi.org/10.5194/bg-8-2317-2011

Frolicher, T. L., Joos, F., Raible, C. C., & Sarmiento, J. L. (2013). Atmospheric CO_2 response to volcanic eruptions: The role of ENSO, season, and variability. *Global Biogeochemical Cycles*, *27*, 239–251. https://doi.org/10.1002/gbc.20028

Frölicher, T. L., Rodgers, K. B., Stock, C. A., & Cheung, W. W. L. (2016). Sources of uncertainties in 21st century projections of potential ocean ecosystem stressors. *Global Biogeochemical Cycles*, *30*, 1224–1243. https://doi.org/10.1002/2015GB005338

Giorgetta, M. A., Jungclaus, J., Reick, C. H., Legutke, S., Bader, J., Böttinger, M., … Stevens, B. (2013). Climate and carbon cycle changes from 1850 to 2100 in MPI-ESM simulations for the Coupled Model Intercomparison Project phase 5. *Journal of Advances in Modeling Earth Systems*, *5*(3), 572–597. https://doi.org/10.1002/jame.20038

Harzallah, A., & Sadourny, R. (1995). Internal versus SST-forced atmospheric variability as simulated by an atmospheric general circulation model. *Journal of Climate*, *8*(3), 474–495. https://doi.org/10.1175/1520-0442(1995)008%3C0474:IVSFAV%3E2.0.CO;2

Hawkins, E., & Sutton, R. (2009). The potential to narrow uncertainty in regional climate predictions. *Bulletin of the American Meteorological Society*, *90*(8), 1095–1107. https://doi.org/10.1175/2009BAMS2607.1

Hedemann, C., Mauritsen, T., Jungclaus, J., & Marotzke, J. (2017). The subtle origins of surface-warming hiatuses. *Nature Climate Change*, *7*(5), 336–339. https://doi.org/10.1038/nclimate3274

Iida, Y., Kojima, A., Takatani, Y., Nakano, T., Midorikawa, T., & Ishii, M. (2015). Trends in pCO_2 and sea-air CO_2 flux over the global open oceans for the last two decades. *Journal of Oceanography*, *71*(6), 637–661. https://doi.org/10.1007/s10872-015-0306-4

Ilyina, T. (2016). Hidden trends in the ocean carbon sink. *Nature*, *530*(7591), 426–427. https://doi.org/10.1038/530426a

Ilyina, T., & Friedlingstein, P. (2016). Carbon feedbacks in the climate system, WCRP Grand Challenge White Paper, 1-10.

Ilyina, T., Six, K., Segschneider, J., Maier-Reimer, E., Li, H., & Núñez-Riboni, I. (2013). The global ocean biogeochemistry model HAMOCC: Model architecture and performance as component of the MPI-Earth System Model in different CMIP5 experimental realizations. *Journal of Advances in Modeling Earth Systems*, *5*, 287–315. https://doi.org/10.1029/2012MS000178

Jungclaus, J. H., Fischer, N., Haak, H., Lohmann, K., Marotzke, J., Matei, D., … von Storch, J. S. (2013). Characteristics of the ocean simulations in the Max Planck Institute Ocean Model (MPIOM) the ocean component of the MPI-Earth system model. *Journal of Advances in Modeling Earth Systems*, *5*, 422–446. https://doi.org/10.1002/jame.20023

Kay, J. E., Deser, C., Phillips, A., Mai, A., Hannay, C., Strand, G., … Vertenstein, M. (2015). The Community Earth System Model (CESM) large ensemble project: A community resource for studying climate change in the presence of internal climate variability. *Bulletin of the American Meteorological Society*, *96*(8), 1333–1349. https://doi.org/10.1175/BAMS-D-13-00255.1

Keller, K. M., Joos, F., & Raible, C. C. (2014). Time of emergence of trends in ocean biogeochemistry. *Biogeosciences*, *11*(13), 3647–3659. https://doi.org/10.5194/bg-11-3647-2014

Kirtman, B., Power, S. B., Adedoyin, J. A., Boer, G. J., Bojariu, R., Camilloni, I., … Wang, H. J. (2013). Near-term climate change: Projections and predictability. In T. F. Stocker, et al. (Eds.), *Climate change 2013: The physical science basis. Contribution of Working Group I to the Fifth Assessment Report of the Intergovernmental Panel on Climate Change* (Chap. 11, pp. 953–1028). Cambridge, UK, and New York: Cambridge University Press.

Landschützer, P., Gruber, N., & Bakker, D. C. E. (2016). Decadal variations and trends of the global ocean carbon sink. *Global Biogeochemical Cycles*, *30*, 1396–1417. https://doi.org/10.1002/2015GB005359

Landschützer, P., Gruber, N., Bakker, D. C. E., & Schuster, U. (2014). Recent variability of the global ocean carbon sink. *Global Biogeochemical Cycles*, *28*, 927–949. https://doi.org/10.1002/2014GB004853

Landschützer, P., Gruber, N., Haumann, F. A., Rödenbeck, C., Bakker, D. C. E., van Heuven, S., … Wanninkhof, R. (2015). The reinvigoration of the Southern Ocean carbon sink. *Science*, *349*(6253), 1221–1224. https://doi.org/10.1126/science.aab2620

Le Quéré, C., Andrew, R. M., Friedlingstein, P., Sitch, S., Pongratz, J., Manning, A. C., … Zhu, D. (2017). Global carbon budget 2017. *Earth System Science Data Discussions*, 1–79. https://doi.org/10.5194/essdd-2017-5123

Le Quéré, C., Raupach, M. R., Canadell, J. G., Marland, G., Bopp, L., Ciais, P., … Woodward, F. I. (2009). Trends in the sources and sinks of carbon dioxide. *Nature Geoscience*, *2*(12), 831–836. https://doi.org/10.1038/ngeo689

Li, H. M., Ilyina, T., Müller, W. A., & Sienz, F. (2016). Decadal predictions of the North Atlantic CO_2 uptake. *Nature Communications*, *7*, 11076. https://doi.org/10.1038/ncomms11076

Li, H. M., & von Storch, J. S. (2013). On the fluctuating buoyancy fluxes simulated in a 1/10 degrees OGCM. *Journal of Physical Oceanography*, *43*(7), 1270–1287. https://doi.org/10.1175/JPO-D-12-080.1

Lovenduski, N. S., McKinley, G. A., Fay, A. R., Lindsay, K., & Long, M. C. (2016). Partitioning uncertainty in ocean carbon uptake projections: Internal variability, emission scenario, and model structure. *Global Biogeochemical Cycles*, *30*, 1276–1287. https://doi.org/10.1002/2016GB005426

Marotzke, J., Jakob, C., Bony, S., Dirmeyer, P. A., O'Gorman, P. A., Hawkins, E., … Tuma, M. (2017). Climate research must sharpen its view. *Nature Climate Change*, *7*(2), 89–91. https://doi.org/10.1038/nclimate3206

McKinley, G. A., Fay, A. R., Lovenduski, N. S., & Pilcher, D. J. (2017). Natural variability and anthropogenic trends in the ocean carbon sink. *Annual Review of Marine Science*, *9*(1), 125–150. https://doi.org/10.1146/annurev-marine-010816-060529

McKinley, G. A., Pilcher, D. J., Fay, A. R., Lindsay, K., Long, M. C., & Lovenduski, N. S. (2016). Timescales for detection of trends in the ocean carbon sink. *Nature*, *530*(7591), 469–472. https://doi.org/10.1038/nature16958

Nevison, C. D., Manizza, M., Keeling, R. F., Stephens, B. B., Bent, J. D., Dunne, J., … Yukimoto, S. (2016). Evaluating CMIP5 ocean biogeochemistry and Southern Ocean carbon uptake using atmospheric potential oxygen: Present-day performance and future projection. *Geophysical Research Letters*, *43*, 2077–2085. https://doi.org/10.1002/2015GL067584

Penduff, T., Juza, M., Barnier, B., Zika, J., Dewar, W. K., Treguier, A. M., … Audiffren, N. (2011). Sea level expression of intrinsic and forced ocean variabilities at interannual time scales. *Journal of Climate*, *24*(21), 5652–5670. https://doi.org/10.1175/JCLI-D-11-00077.1

Peters, G. P., Le Quéré, C., Andrew, R. M., Canadell, J. G., Friedlingstein, P., Ilyina, T., … Tans, P. (2017). Towards real-time verification of CO_2 emissions. *Nature Climate Change*, *7*(12), 848–850. https://doi.org/10.1038/s41558-017-0013-9

Popp, M., Schmidt, H., & Marotzke, J. (2016). Transition to a moist greenhouse with CO_2 and solar forcing. *Nature Communications*, *7*. https://doi.org/10.1038/ncomms10627

Reick, C. H., Raddatz, T., Brovkin, V., & Gayler, V. (2013). Representation of natural and anthropogenic land cover change in MPI-ESM. *Journal of Advances in Modeling Earth Systems*, *5*(3), 459–482. https://doi.org/10.1002/jame.20022

Resplandy, L., Séférian, R., & Bopp, L. (2015). Natural variability of CO_2 and O_2 fluxes: What can we learn from centuries-long climate models simulations? *Journal of Geophysical Research: Oceans*, *120*, 384–404. https://doi.org/10.1002/2014JC010463

Ritter, R., Landschützer, P., Gruber, N., Fay, A. R., Iida, Y., Jones, S., … Zeng, J. (2017). Observation-based trends of the Southern Ocean carbon sink. *Geophysical Research Letters*, *44*. https://doi.org/10.1002/2017GL074837

Rödenbeck, C., Bakker, D. C. E., Gruber, N., Iida, Y., Jacobson, A. R., Jones, S., … Zeng, J. (2015). Data-based estimates of the ocean carbon sink variability first—Results of the Surface Ocean pCO_2 Mapping intercomparison (SOCOM). *Biogeosciences*, *12*(23), 7251–7278. https://doi.org/10.5194/bg-12-7251-2015

Rödenbeck, C., Keeling, R. F., Bakker, D. C. E., Metz, N., Olsen, A., Sabine, C., & Heimann, M. (2013). Global surface-ocean pCO_2 and sea-air CO_2 flux variability from an observation-driven ocean mixed-layer scheme. *Ocean Science*, *9*(2), 193–216. https://doi.org/10.5194/os-9-193-2013

Rodgers, K. B., Lin, J., & Frolicher, T. L. (2015). Emergence of multiple ocean ecosystem drivers in a large ensemble suite with an Earth system model. *Biogeosciences*, *12*(11), 3301–3320. https://doi.org/10.5194/bg-12-3301-2015

Schuster, U., & Watson, A. J. (2007). A variable and decreasing sink for atmospheric CO_2 in the North Atlantic. *Journal of Geophysical Research*, *112*, C11006. https://doi.org/10.1029/2006JC003941

Séférian, R., Ribes, A., & Bopp, L. (2014). Detecting the anthropogenic influences on recent changes in ocean carbon uptake. *Geophysical Research Letters*, *41*, 5968–5977. https://doi.org/10.1002/2014GL061223

Segschneider, J., Beitsch, A., Timmreck, C., Brovkin, V., Ilyina, T., Jungclaus, J., … Zanchettin, D. (2013). Impact of an extremely large magnitude volcanic eruption on the global climate and carbon cycle estimated from ensemble Earth System Model simulations. *Biogeosciences*, *10*(2), 669–687. https://doi.org/10.5194/bg-10-669-2013

Stevens, B. (2015). Rethinking the lower bound on aerosol radiative forcing. *Journal of Climate*, *28*(12), 4794–4819. https://doi.org/10.1175/JCLI-D-14-00656.1

Stevens, B., Giorgetta, M., Esch, M., Mauritsen, T., Crueger, T., Rast, S., … Roeckner, E. (2013). Atmospheric component of the MPI-M Earth System Model: ECHAM6. *Journal of Advances in Modeling Earth Systems*, *5*, 146–172. https://doi.org/10.1002/jame.20015

Suárez-Gutiérrez, L., Li, C., Thorne, P. W., & Marotzke, J. (2017). Internal variability in simulated and observed tropical tropospheric temperature trends. *Geophysical Research Letters*, *44*, 5709–5719. https://doi.org/10.1002/2017GL073798

Takahashi, T., Sutherland, S., & Kozyr, A. (2014). Global ocean surface water partial pressure of CO_2 database: Measurements performed during 1957–2013 (version 2013), ORNL/CDIAC-160, NDP-088(V2013), Carbon Dioxide Information Analysis Center, Oak Ridge National Laboratory, U.S. Department of Energy, Oak Ridge, Tennessee.

Tebaldi, C., & Knutti, R. (2007). The use of the multimodel ensemble in probabilistic climate projections. *Philosophical Transactions of the Royal Society A*, *365*(1857), 2053–2075. https://doi.org/10.1098/rsta.2007.2076

Thomas, H., Prowe, A. E. F., Lima, I. D., Doney, S. C., Wanninkhof, R., Greatbatch, R. J., … Corbiere, A. (2008). Changes in the North Atlantic Oscillation influence CO_2 uptake in the North Atlantic over the past 2 decades. *Global Biogeochemical Cycles*, *22*, GB4027. https://doi.org/10.1029/2007GB003167

Ting, M., Kushnir, Y., Seager, R., & Li, C. (2009). Forced and internal twentieth-century SST trends in the North Atlantic. *Journal of Climate*, *22*(6), 1469–1481. https://doi.org/10.1175/2008JCLI2561.1

United Nations Framework Convention on Climate Change (2015). Adoption of the Paris agreement—by the President—Draft decision-/CP.21, UNFCCC. 12 December 2015.

van Vuuren, D. P., Edmonds, J., Kainuma, M., Riahi, K., Thomson, A., Hibbard, K., … Rose, S. K. (2011). The representative concentration pathways: An overview. *Climatic Change*, *109*(1-2), 5–31. https://doi.org/10.1007/s10584-011-0148-z

Wang, L., Huang, J., Luo, Y., & Zhao, Z. (2016). Narrowing the spread in CMIP5 model projections of air-sea CO_2 fluxes. *Scientific Reports*, *6*(1), 37548. https://doi.org/10.1038/srep37548

Zhou, T., & Yu, R. (2006). Twentieth century surface air temperature over China and the globe simulated by coupled climate models. *Journal of Climate*, *19*(22), 5843–5858. https://doi.org/10.1175/JCLI3952.1